RESEARCH ARTICLE

WILEY

Effect of flow ramping on stranding potential related to river morphology—Developing hydraulic indices for peaking severity

Knut Alfredsen [ORCID] | Mulubirhan Gebretsadik Tekle

Department of Hydraulic and Environmental Engineering, Norwegian University of Science and Technology, Trondheim, Norway

Correspondence
Knut Alfredsen, Department of Hydraulic and Environmental Engineering, Norwegian University of Science and Technology, Trondheim 7491, Norway.
Email: knut.alfredsen@ntnu.no

Abstract

Stranding can be an important negative effect downstream of peaking power plants. Much work is put into computing indices of peaking operation based on flow data from power plant outlets or in reaches downstream of power plants. Such indices give good measures of the frequency and magnitude of hydropeaking and indirectly the potential severity of the operation. To address stranding potential local studies are needed to find measures that relate river geometry to dewatered areas and dewatering speeds and the length of river downstream that is affected by the power plant operation. In recent years, high-precision laser scans have become available for some Norwegian rivers making it possible to do hydraulic modeling on a scale that can describe the dewatering process in detail. The new data also provides details on the river valley and areas adjacent to the rivers. Using these data, we have carried out simulations for peaking operations in several rivers and computed indices of hydraulic effects of potential shutdown hydrographs. The results show a dampening effect in all rivers and a significant relationship between river features like distance from outlet and cross section geometry and the hydraulic dependent indices ramping rate and dewatering rate. These relations could be a method for initial assessment of the effect of hydropeaking on rivers and a foundation for deciding on where more detailed studies will be needed.

KEYWORDS
hydraulic modeling, hydropeaking, ramping rate, river geometry, stranding

1 | INTRODUCTION

Hydropower provides a high degree of flexibility in production and is therefore suitable for balancing variable demand in the energy market. Particularly when combined with reservoir storage, the flexibility of the hydropower systems is seen as an important component in the transition to a renewable energy system through balancing intermittent energy sources like wind and sun. The operation of hydropower as a source of load balancing will lead to frequent variations in turbine load and thereby water flow through the hydropower plant and therefore also flow fluctuations downstream of the power plant outlet. This is particularly important when the outlet is in a downstream river since it can cause rapid changes in water level with corresponding rapid changes in wetting–drying of the riverbed along the margins of the river. This operation is frequently referred to as hydropeaking, and the rate of change of flow is commonly outside what is observed in the natural hydrograph (Greimel et al., 2016). With increasing need for flexibility in the power system, hydropeaking is expected to

increase in the future example as shown by Ashraf et al. (2018) for the Nordic region. Several studies exist in literature of the effect of flow ramping on the environment and cover a number of topics like stranding of fish due to rapid dewatering of the river bed and seasonal differences (Saltveit et al., 2001; Saltveit et al., 2020), movements and home ranges during peaking (Berland et al., 2004; Scruton et al., 2008), impacts on invertebrates (Bruno et al., 2013), impacts on riparian vegetation (Bejarano, Jansson, & Nilsson, 2017), and impacts on fish communities (Schmutz et al., 2015). Mitigation measures are proposed and related to flow management, channel modifications, and compensation measures (Charmasson & Zinke, 2011). This is exemplified by Hayes et al. (2019), who propose flow mitigation measures targeted at fish life stages and show the need for variable mitigation measures dependent on season and life stage.

Several methods are described to investigate hydropeaking in rivers. Carolli et al. (2015) and Sauterleute and Charmasson (2014) describe methods to detect peaking operation from analysis of time series of discharge downstream of hydropower plants. Greimel et al. (2016) present a general framework for discharge analysis that can classify different types of flow fluctuation including hydropeaking and small amplitude artificial fluctuations termed hydro fibrillations. Several methods aimed at describing changes in the operations of power plants through analysis of regulated and unregulated time series have also been developed (e.g., Bejarano et al., 2020; Bejarano, Sordo-Ward, et al., 2017; Bevelhimer et al., 2014). The above methods provide indices describing hydrological alterations due to hydropeaking and are used to evaluate aspects of flow changes over time. Such indicators can be related to impacts on fish populations (Schmutz et al., 2015), and there are methods developed that link physical descriptions as described above with biological measures to measure the impact of peaking on fish populations (e.g., Bakken et al., 2021), who combines measures of altered discharge and wetted areas with factors describing the vulnerability of Atlantic salmon to develop an index relating hydropeaking to Atlantic salmon populations. Vertical ramping rates have also been used to set requirements for hydropower operation (Halleraker et al., 2022; Moreira et al., 2019), and are currently used to limit hydropeaking in several Norwegian hydropower licenses. Lateral connectivity is also important for stranding, and the slope of bars can influence the stranding rate (Hauer et al., 2014), and tools to assess connectivity and stranding potential are proposed (Larrieu et al., 2020; Le Coarer et al., 2022). The lateral drying rate or horizontal drying rate is also an important factor for the stranding of fishes (Hauer et al., 2023; Le Coarer et al., 2022). Common for the lateral drying rate and the dewatered area is that it cannot be derived from hydrological data alone but also needs the river geometry as an input in the computation. It is therefore necessary to know the shape of the transect where these parameters are to be computed. Further, all stranding indices will vary as we move from the outlet, influenced by the morphology and the natural dampening effects in the river (Hauer et al., 2014; Hauer et al., 2017). In the method presented by Bakken et al. (2021), two ways of measuring the effect of rapid flow fluctuations on physical changes in the river

are proposed, the vertical dewatering rate (cm/h) and the change in dewatered area (%) of the affected river reach. The latter is the result of the lateral during rate as described above. These two factors are considered important for assessing the potential effects of hydropeaking in a river, for example, stranding of fish and invertebrates, and are controlled by the variability of the cross-sectional shape of the river as we move downstream from the outlet of the hydropower plant. Studying longitudinal impacts of peaking would require hydraulic modeling of long river reaches to assess both vertical and lateral ramping rates, and a detailed computation of dewatering would further require detailed geometry data to properly assess dewatered areas. Casas-Mulet et al. (2014) used a one-dimensional (1D) model to simulate dewatering in a 2.5 km long river reach and provided guidelines on the needed cross section density for computing correct stranding areas compared to field observations. For stranding assessment, a 1-D approach would need a denser set of cross section than for traditional water level or flood assessment thereby needing extra field work. Casas-Mulet et al. (2014) also show that the needed density of cross sections increases in more complex geometries, also adding to the needed field work. Vanzo et al. (2016) used a 2D hydraulic model to simulate wetted areas and dewatering rates along the same reach as in Casas-Mulet et al. (2014). The 2D approach provided a more detailed description of the reach and thereby also a better prediction of the dewatered areas compared to the 1D approach. Hauer et al. (2014) used a 2D hydraulic model and habitat modeling to estimate stranding risk for juvenile brown trout over a range of different hydro morphological units and found significant effects of channel bar form on stranding risk. The authors also show the importance of substrate size in relation to stranding areas. The effect of distance from the outlet on changes in ramping rate is also shown by Hauer et al. (2017) who used numerical modeling to describe changes in longitudinal vertical ramping rate for the planning of mitigation measures.

In recent years, high-precision laser scans using bathymetric (green) LiDAR (Mandlburger et al., 2015) have become available for several Norwegian rivers (Awadallah et al., 2022), which in combination with efficient 2D hydraulic models makes it possible to describe the dewatering process with a high level of detail over longer river reaches (e.g., Juarez et al., 2019). Combined with topographic LiDAR scans of the adjacent terrain, we can develop digital elevation models (DEMs) covering both the river bathymetry and the areas adjacent to the rivers which provides a full description of the river profile and potential stranding areas. Since entire rivers are mapped with LiDAR, we can compute detailed hydropeaking indices based on hydraulic modeling both longitudinally and transverse for large areas and thereby cover several different river geometries. This will improve the accuracy compared to studies based on coarser terrain models or cross-sectional-based 1D models since getting similar accuracy in bathymetry is difficult if not impossible with other field measurement techniques. Recently, Bürgler et al. (2022) have shown that a detailed 2D model is better than a detailed 1D model for habitat assessment, and also for computing dewatering speeds and wetted areas for more complex river morphologies. Stickler et al. (2023) show that going

from 16 to 0.01 points per m² reduces the accuracy in areal prediction in a 2D hydraulic model, indicating that the high detail available in the LiDAR dataset will improve the prediction of wetted areas in hydropeaking studies.

The main objective of this paper is to investigate the relation between hydropeaking severity and river features with an objective to find a method for assessing potential ramping effects in rivers where data for detailed studies are not available. We use detailed LiDAR bathymetry and hydraulic modeling to compute two hydropeaking indices, namely the vertical ramping rate and the lateral drying rate for three different Norwegian rivers. Further, we computed a series of river descriptors describing the river geometry for each river and evaluated the relation between the hydropeaking indices and river descriptors using statistical models, with an objective to find relations that can be used to classify the potential hydropeaking severity in rivers with less detailed data available for hydraulic simulations.

2 | MATERIALS AND METHODS

2.1 | Study sites

Three rivers in Norway were used for the study (Figure 1). Lærdalselva (61.10° N, 7.48° E) is a gravel bed river that flows from the Filefjell mountains to the sea at Lærdalsøyri, and in this study we have used the lowest 16 km from Stuvane to the sea. Eidselva (61.90° N, 5.98° E) is a gravel bed river that flows from Lake Hornindalsvatn to the sea, a distance of 9.2 km. For Storåne (60.6° N,8.21° E), we have used the 2.5 km reach from the outlet of the Hol 1 power plant to Lake Hovsfjorden. Storåne is also a gravel-bed river with a braided channel.

All rivers had full coverage of bathymetric LiDAR data from aerial measurements from airplanes. Based on the point clouds from the LiDAR flights, DEMs were interpolated with a resolution of 0.5 × 0.5 m using ArcMap version 10.8. For Lærdalselva and Eidselva which do not have power plants that carry out hydropeaking, ramping
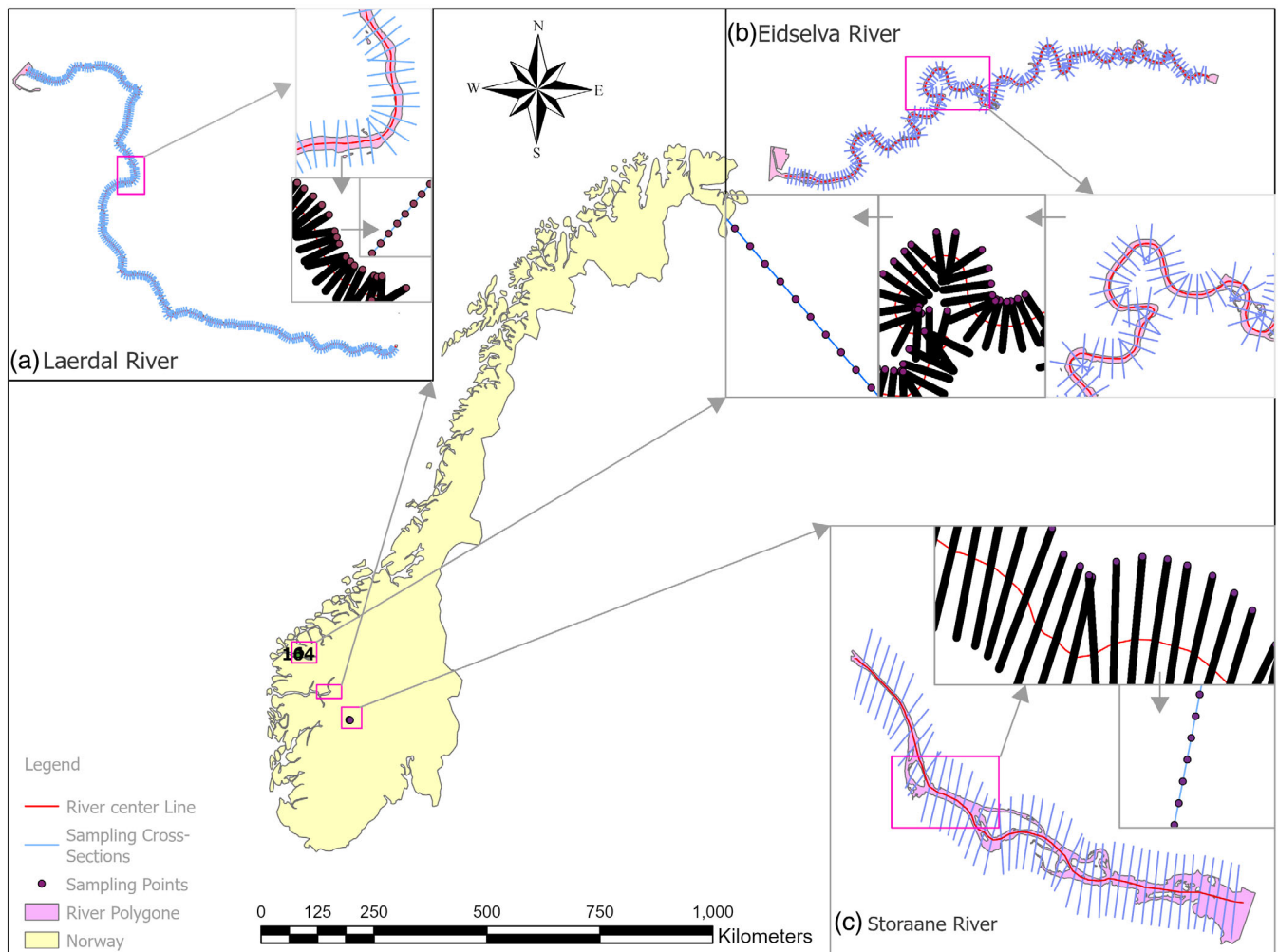

FIGURE 1 Map of study sites. The panels show Lærdalselva (a), Eidselva (b), and Storåne (c). Each panel shows the full set of cross sections, a zoomed view of the cross sections and an example of the points along the cross sections used for computing the hydropeaking indices. [Color figure can be viewed at wileyonlinelibrary.com]

regimes that are realistic in size but not related to any operating plant were used, while for Storåne we used a ramping rate corresponding to a shutdown of the Hol 1 power plant (Juarez et al., 2019).

2.2 | Hydraulic simulations and extraction of hydropeaking indices

The hydraulic simulations were carried out using the 2D version of the Hydrologic Engineering Centre's River Analysis System (HEC-RAS) v.6 (Brunner, 2021). For Storåne, a model developed and calibrated for hydropeaking analysis by Juarez et al. (2019) was used and for Lærdal a model set up and calibrated by Alfredsen et al. (2019) was used. For Eidselva, a model was set up and calibrated against the water edge from georeferenced aerial images. We used aerial imagery from the repository of the Norwegian mapping authority (www. norgeibilder.no). From the metadata of the images the time of flight

was recorded, and we could use this to extract the discharge in the image from the NVE gaging station "Eidselva ndf. Hornindal" (89.2.0). A Manning region layer was created and used to calibrate the model to reproduce the wetted areas of the images. The calibrated models were then used to simulate the flow ramping scenario from Table 1.

Raster maps of depth, velocity, and the inundation boundary were extracted from the HEC-RAS simulations with a time interval of 1 min. Raster maps were then imported into ArcGIS Pro version 2.9.1 (www. esri.com), and cross sections were generated for every 50 m along the centerline of the river (Figure 2a), and from the cross sections, the hydraulic variables (water-covered area, water level, and discharge) were extracted for every 20 cm on a time interval of 1 min and stored using a script written in Python and ArcPy. In addition, we computed the longitudinal slope between cross sections, the distance from the power plant outlet and the transverse slope (TS) of the dewatered area. The TS of each cross section was computed by dividing the elevation difference between points distributed with an

TABLE 1 Key data for the rivers used in the analysis.

River	Length (km)	Ramping (m^{3}s^{-1})	Stop time (min)	Min-max ratio	DEM (m)	Model grid
Eidselva	9	40–5	10	8	0.5 × 0.5	5 × 5
Lærdalselva	15	55–10	10	5.5	0.35 × 0.35	5 × 5
Storåne	2.5	66–6	10	11	0.5 × 0.5	1 × 1

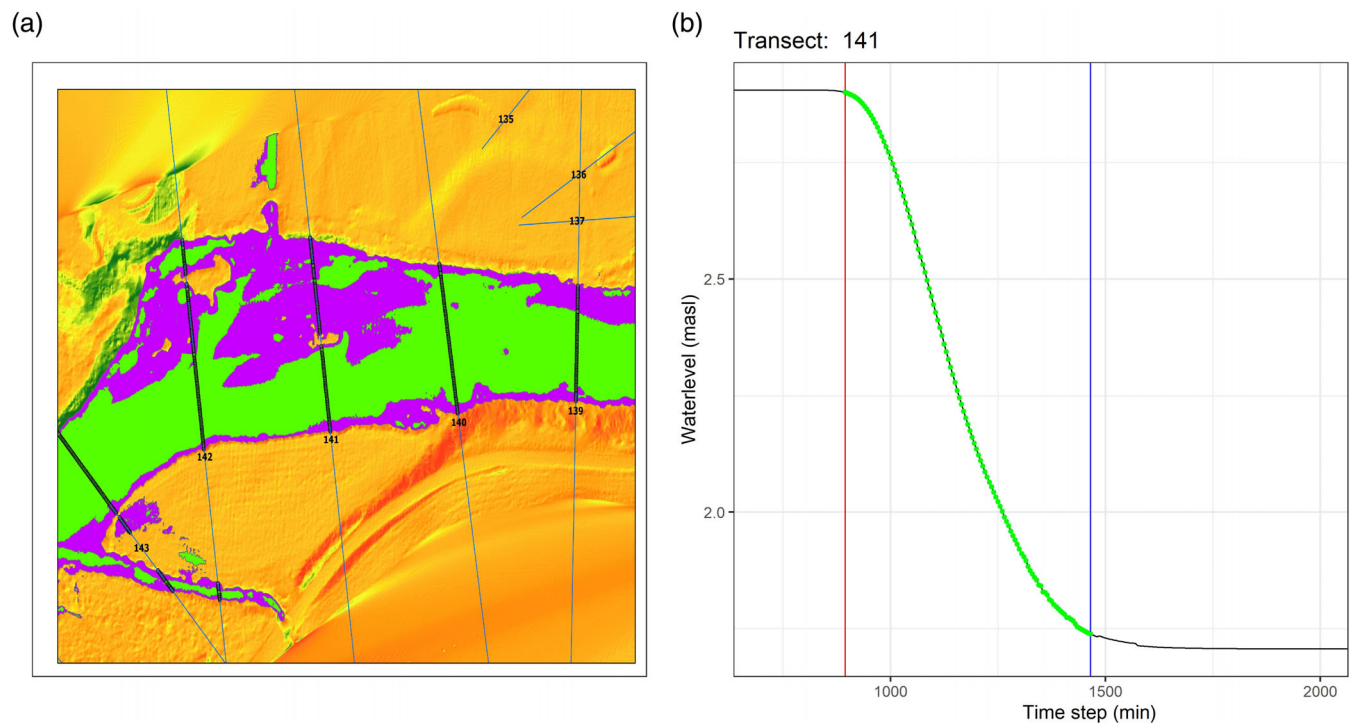Abbreviation: DEM, digital elevation model.

FIGURE 2 Cross sections (a) and an example of an identified down-ramping event from the hydrograph (b) from Eidselva. In panel (a), the pink color shows the areas dried out from full to low flow and the black lines are the cross sections used in the analysis. Panel (b) shows the shutdown hydrograph, the red vertical line shows the identified start and the blue vertical line is the identified end of the hydrograph. The green dots show the points where the ramping indices are sampled. [Color figure can be viewed at wileyonlinelibrary.com]

interval of 20 cm across the cross section with the distance between those points (L), and then the mean, median, and standard deviation of the slope were computed for the part of the cross section dried out during the peaking operation. The slope is expressed as a fraction ranging from 0 to 1, where a low value indicates a mild slope TS is calculated by the following equation.

$$TS = \frac{Y_{n+1} - Y_n}{L}, \quad (1)$$

where Y is the elevation of the point and L is the horizontal distance between the points. This way the variation of cross section slopes across the river was captured for further analysis of the relation between hydropeaking indices and cross section geometry. To analyze the hydropeaking indices, we extracted the water level (WSE) at an interval of 20 cm across the cross section for each unsteady flow profile with a 1-min time resolution. We then calculated the average water level for every cross section at every time step. For each cross section in the dataset, we identified the start and end of the down-ramping event (Figure 2b). The vertical ramping rate is computed as the drop in water level between the start and end of the down-ramping event, divided by the time it takes from stable high flow to stable low flow (Equation 2). In addition, we also computed the vertical ramping rate for each ramping interval with a resolution of 1-min for each cross section.

$$rr = \frac{\text{Water level at full flow} - \text{Water level at low flow (cm)}}{dt\,(\text{minute})}. \quad (2)$$

To compute the lateral drying rate, we extracted wetted width at 1-min interval for each cross section. The dried-out width was computed as the difference in wet width between the start and the end of the down-ramping events. From the wetted width, the lateral drying rate was computed as the rate of change in dried-out width with time using (Equation 3). The lateral drying rate for each ramping interval with a resolution of 1-min for each cross section was also computed.

$$ldr = \frac{\text{Wet width at fullflow} - \text{wet width at low flow (metre)}}{dt\,(\text{min})}. \quad (3)$$

The dried-out percentage was computed for each cross section as

$$\text{Dry percentage} = \frac{\text{Wet width at full flow} - \text{wet width at low flow(metre)}}{\text{width at fullflow}} \ast 100. \quad (4)$$

2.3 | Data analysis

To investigate the relationship between the river descriptors and the hydropeaking indices linear and non-linear regression analysis were carried out. We used two hydropeaking indices and river descriptors

TABLE 2 Response and predictor variables used in the statistical analysis.

Response variables	
Vertical ramping rate (cm/min)	**Vertical reduction in water level at a cross section**
Lateral ramping rate (cm/min)	Drying rate of cross section
Predictor variables	
River width (m)	The river width at full flow
Distance from outlet (km)	The distance from the outlet measured along river centerline
Mean cross-sectional slope (−)	The mean of the cross-sectional slope (Equation 1)
Median cross-sectional slope (−)	The median of the cross-sectional slope
Standard deviation of cross-sectional slope (−)	The standard deviation of the cross-sectional slope, used as a measure of the variability of slopes in the river
Longitudinal slope (−)	Longitudinal slope between cross sections
Dried out length of cross section (m)	Difference between wetted width at high and low flow
Width to depth ratio (−)	Wetted width divided by depth at full flow

(Table 2). For each analysis, we evaluated the effect of adding descriptor values to the regression by assessing the goodness of fit of the model and the significance level ($\alpha = 0.05$) of the variable added.

The analysis was first carried out for each individual river to see if relationships existed and to see the variation across rivers with different features. To see if we can generalize this relationship, we pooled all data into one dataset and carried out a similar analysis on data from all rivers. Since the rivers are of different lengths, we also did an analysis on the pooled dataset where we only used the data corresponding to the shortest river.

Comparison of hydropeaking indices and river descriptors between the study sites was done using Kruskal–Wallis and Pairwise Wilcoxon tests. We used both linear and non-linear regression for the evaluation of the relations between hydropeaking indices and river descriptors, and we used a mixed model approach to test the effect of the individual rivers in the pooled dataset. All analysis was done using the R statistical software (R Core Team, 2019) using nls.multstart (Padfield & Matheson, 2020), lme4 (Bates et al., 2015), and ggplot2 (Wickham, 2016) packages.

3 | RESULTS

By extracting the time of flight from the metadata of aerial images we could find the discharge which was then simulated. The water-covered area was extracted from the simulation and overlaid the aerial images in the GIS (Figure 3). We then used visual inspection to assess

FIGURE 3   Comparison of simulated (blue transparent surface) with aerial imagery for the hydraulic simulation of Eidselva. *Source*: aerial imagery www.norgeibilder.no, *Courtesy*: Statkart and the Geovekst project. [Color figure can be viewed at wileyonlinelibrary.com]

the accuracy of the hydraulic model and as a basis for adjusting the calibration until we had an acceptable match between the simulated and observed water-covered area.

A set of descriptors describing the river features and some effects of changes in flow are shown in Figure 4 for each study river. For factors that potentially will influence the dewatering rate of the riverbed, the cross-sectional slopes are significantly different in Storåne compared to Lærdal and Eidselva ($p < 0.05$), while there is no significant difference between Lærdal and Eidselva. The longitudinal slope is not significantly different between any of the rivers ($p > 0.05$), but Lærdal and Storåne have some steeper sections than Eidselva as seen in the outliers. The river width is also significantly different in Storåne compared with Lærdal and Eidselva, while no significant difference is seen between Lærdal and Eidselva. This shows that Storåne is wider and has milder cross-sectional slopes than the two other rivers, which is mostly due to the widening in the lower part of the river where the rivers enter the Hovsfjorden lake.

The hydrograph for the shutdown in Eidselva is computed for each cross-section and the result for selected cross sections from the top to the bottom of the river is shown in Figure 5. We see a gradual downstream dampening of the wave as we progress downstream in the river. The time from full flow to low flow is increasing and the slope of the falling limb of the hydrograph is becoming milder. For Eidselva, the time from full to low flow at cross section 5 is 17 min (250 m from the outlet), and the time from full to low flow in cross

section 175 which is 8.75 km from the outlet is 134 min. For Lærdalselva the time from full to low flow for cross section 5 is 25 min and for the lower part of the river (cross section 305, 15.25 km from the outlet) the time is 190 min. For Storåne the shutdown time is 24 min in cross section 5 and for cross section 45 (2.25 km from the outlet) the shutdown time is 79 min. The shutdown times are computed from the time the river starts to drop and until the hydrograph is completely flat after the drop thereby including some periods with small changes in both ends.

The computed ramping rate (cm/min) and drying rate (cm/min) are computed for each cross section and for each ramping interval with a resolution of 1 min. The result is shown for Eidselva in Figure 6. Here the boxplot with outliers shown in the upper panel represents the variation in vertical ramping rate computed for each 1-min interval during the shutdown, and in the lower panel, we see a similar plot of the lateral drying rate. The average value is also marked on each plot. We can see that both the variability and size of the vertical ramping rate are reduced as we move downstream from the outlet due to the natural dampening in the river reaches. The variation in the value of the ramping rate relates to the slope of the hydrograph which is flatter in the beginning and end and steepest in the middle (see Figure 2). The pattern of reduction of the ramping rate is seen for all three study sites, but we can also see that the value of the ramping rate is different in the three rivers and that the final value is different as the rivers have different lengths and thereby different levels of
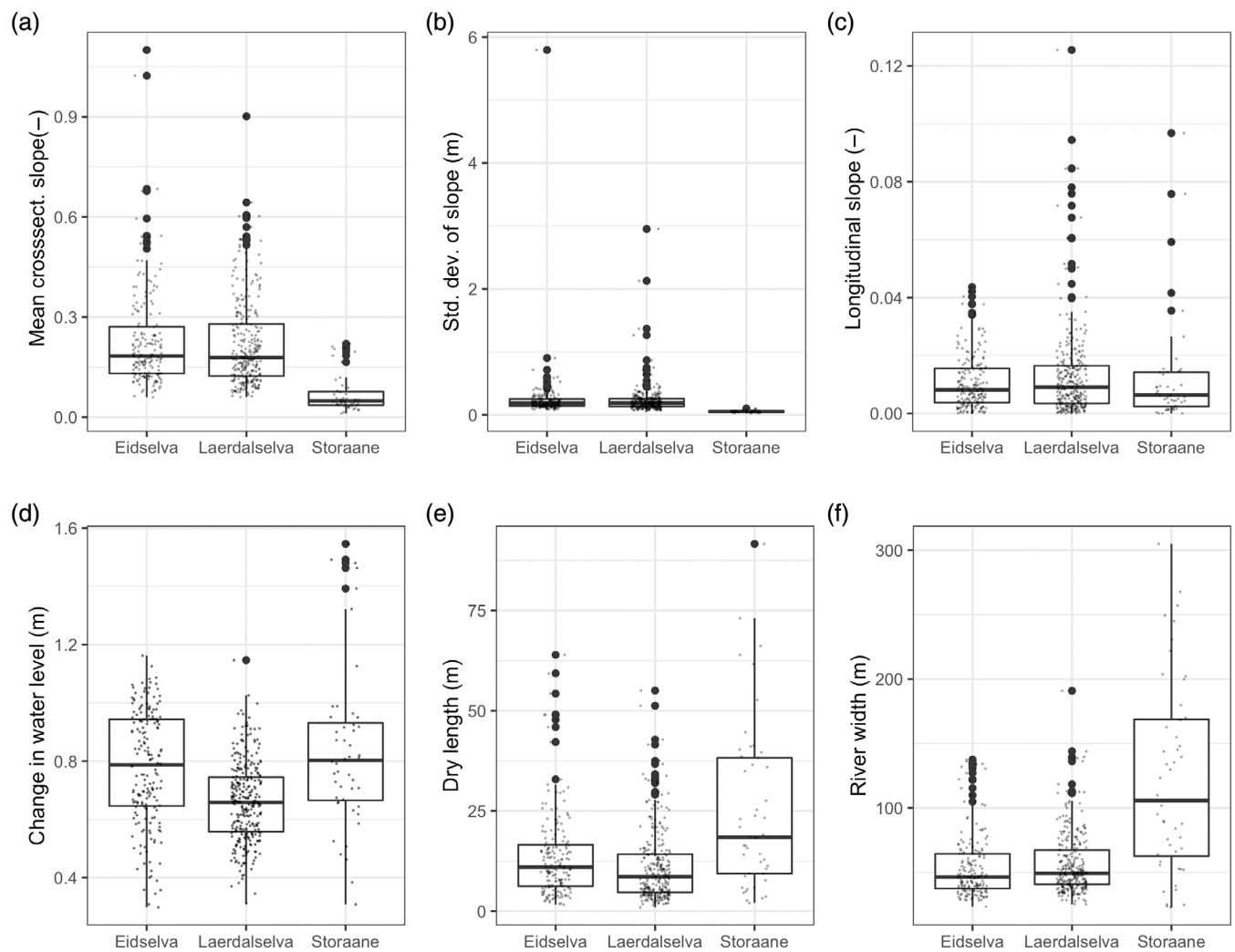
FIGURE 4 River characteristics from the study sites. (a) Mean lateral cross section slope, (b) standard deviation of the lateral cross section slope, (c) Longitudinal slope between cross sections, (d) Change in water level, (e) Dry length of cross sections at low flow, and (f) Total cross section width. Boxes represent the inner quartile and the horizontal line is the median value, the gray points show the distribution of data for each river.

dampening. The lateral drying rate shows no relation to the distance from the outlet and has a larger variability along the river reach. For all study sites, we see that high levels of vertical and lateral drying can occur at different locations along the river reaches, which is important for the evaluation of hydropeaking impacts.

A summary of the main hydropeaking indices for the three rivers is shown in Figure 7. Here, we have also computed the dry area percentage as used in Bakken et al. (2021) as a criterion for hydropeaking severity.

The results show that all rivers have stranding indices that are above the limits as described by Bakken et al. (2021) for the shutdown regime applied to the three study reaches. For the ramping rate, we find a significant difference between all rivers, Eidselva and Lærdal and Lærdal and Storåne ($p < 0.001$), while Storåne and Eidselva ($p = 0.013$). For the lateral drying rate, we find a significant difference between all rivers ($p < 0.001$). For the dried percentage of the profile, we see a significant difference between Eidselva and Lærdal

($p < 0.001$) while there is no significant difference in the other comparisons.

In Figure 8a, the vertical ramping rate computed using Equation 2 is plotted against the distance from the outlet for the three study sites. For all cases, a relationship between the distance from the outlet and the ramping rate was found by fitting a regression line to log-transformed data. We do see a significant relationship ($p < 0.001$) and find R^2 values of 0.75, 0.87, and 0.84 for Lærdalselva, Eidselva, and Storåne, respectively.

In Figure 8b, we see that the relationship observed at each of the study sites also is significant for the pooled data ($p < 0.001$, R^2 for the regression line 0.78). The fitted regression line and the non-linear regression give similar results except for the linear regression overestimating the vertical ramping rate at the outlet location.

Adding river width as a second explanatory variable is significant ($p < 0.001$) and increased the R^2 to 0.81, indicating that the river width also contributes to the ramping rate. Adding the dry length of
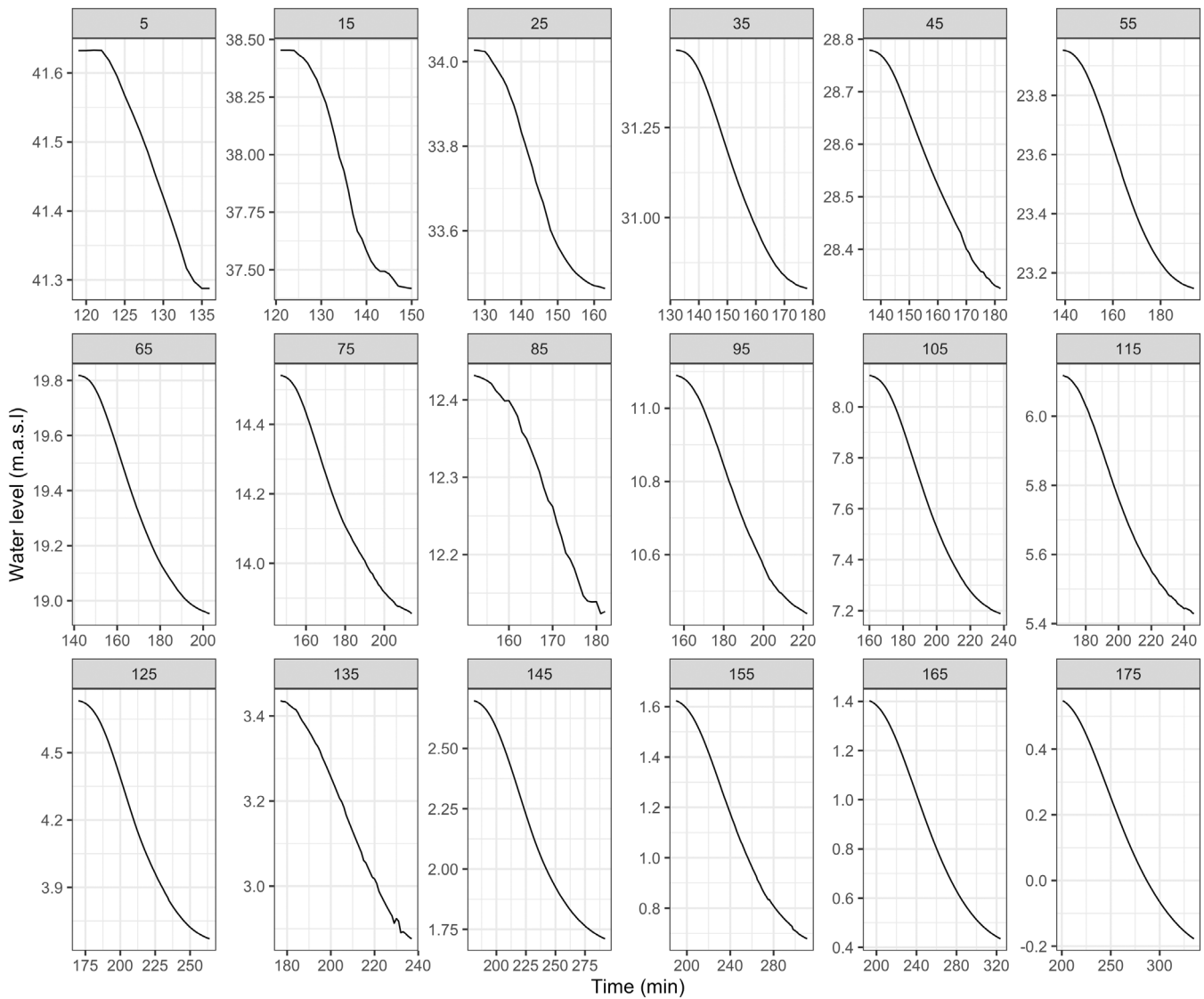
FIGURE 5 The propagation of shutdown hydrographs in Eidselva identified by cross section numbers. The lowest number is closest to the outlet and the distance from the outlet is found by multiplying the cross-section number with 50 m. Similar plots for Storåne and Lærdalselva are shown in Figures S1 and S2.

the section is also significant and adds an extra percentage point to the R^2. The dry length is also correlated with the river width and conveys some of the same information, in addition is a variable that is difficult to estimate without a hydraulic model. The mean transverse cross-sectional slope has a weak significance in the result ($p = 0.011$) but shows no increase in goodness of fit, while the longitudinal slope is not significant for predicting the vertical ramping rate. Adding interaction between the explanatory variables did not improve the relationship. With three different rivers pooled together, an effect of the river on the relationship could be an option. Adding the river as a random effect to the regression did not improve the result.

Unlike the vertical ramping rate, the lateral drying rate is not very much influenced by the dampening as we move downstream in the river (Figure 6) and the distance from the outlet does not give any explanation for the variation in drying rate. The rate of drying in a

river section will have a relation to the side slope of the terrain and is represented by the mean slope of the cross section. In Figure 9a, we see the lateral drying rate for the three rivers as a function of the mean slope in each cross section. The regression line shows a reasonable fit, with a goodness of fit of 0.55, 0.51, and 0.52 for Eidselva, Lærdalselva, and Storåne, respectively.

Pooling the data together the relationship between the mean cross-sectional slope and the lateral drying rate is maintained when the regression is carried out on the log-transformed data ($p < 0.001$, $R^2 = 0.55$). Fitting a non-linear regression model to the data gives a similar fit as the regression line, but we see an overestimation for the cross sections with the mildest slopes in the log-transformed regression model (Figure 9b).

Adding river width as a second explanatory variable to the pooled dataset provides no significant contribution to the model ($p = 0.53$)
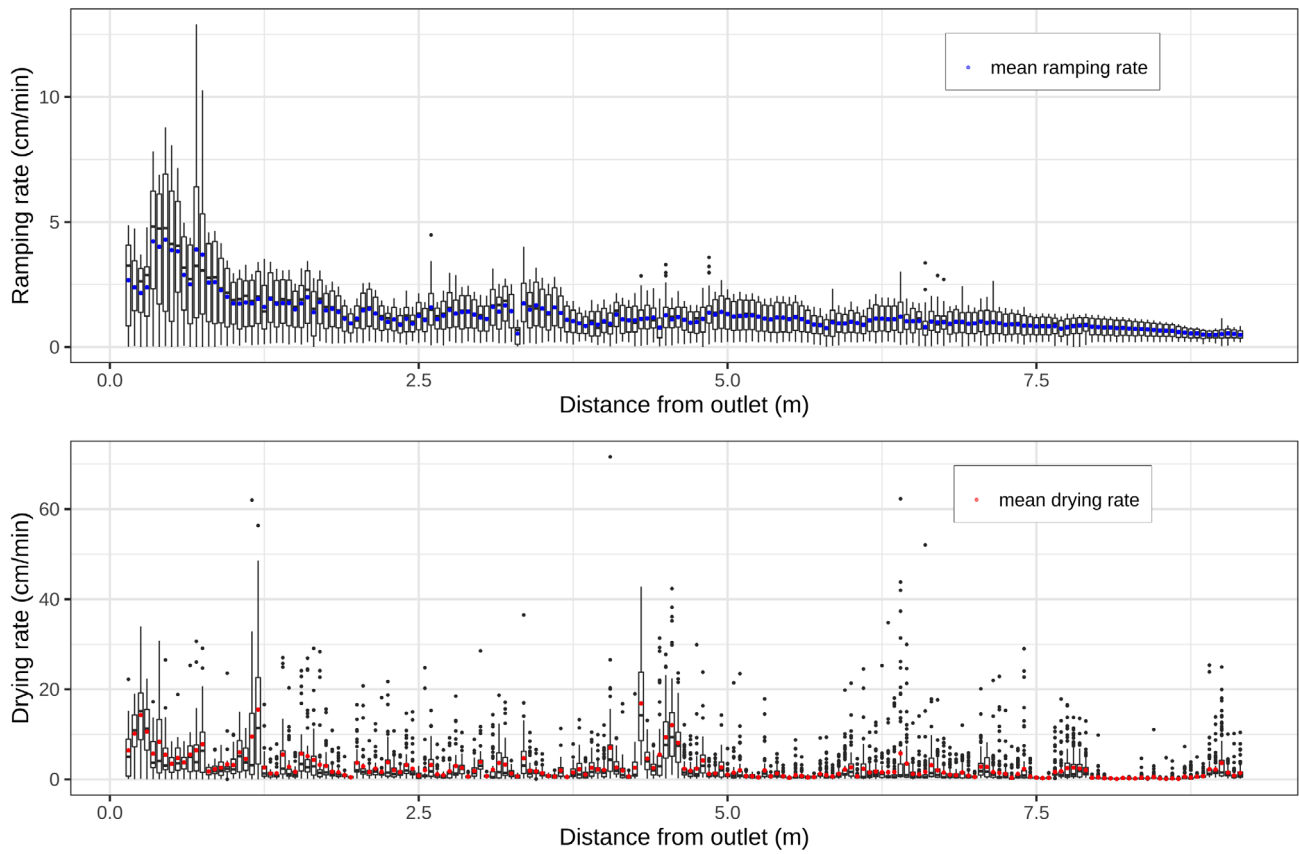
FIGURE 6 Detailed view of peaking indices for Eidselva. Upper panel ramping rate and lower panel lateral drying rate. The unit is cm/min. [Color figure can be viewed at wileyonlinelibrary.com]
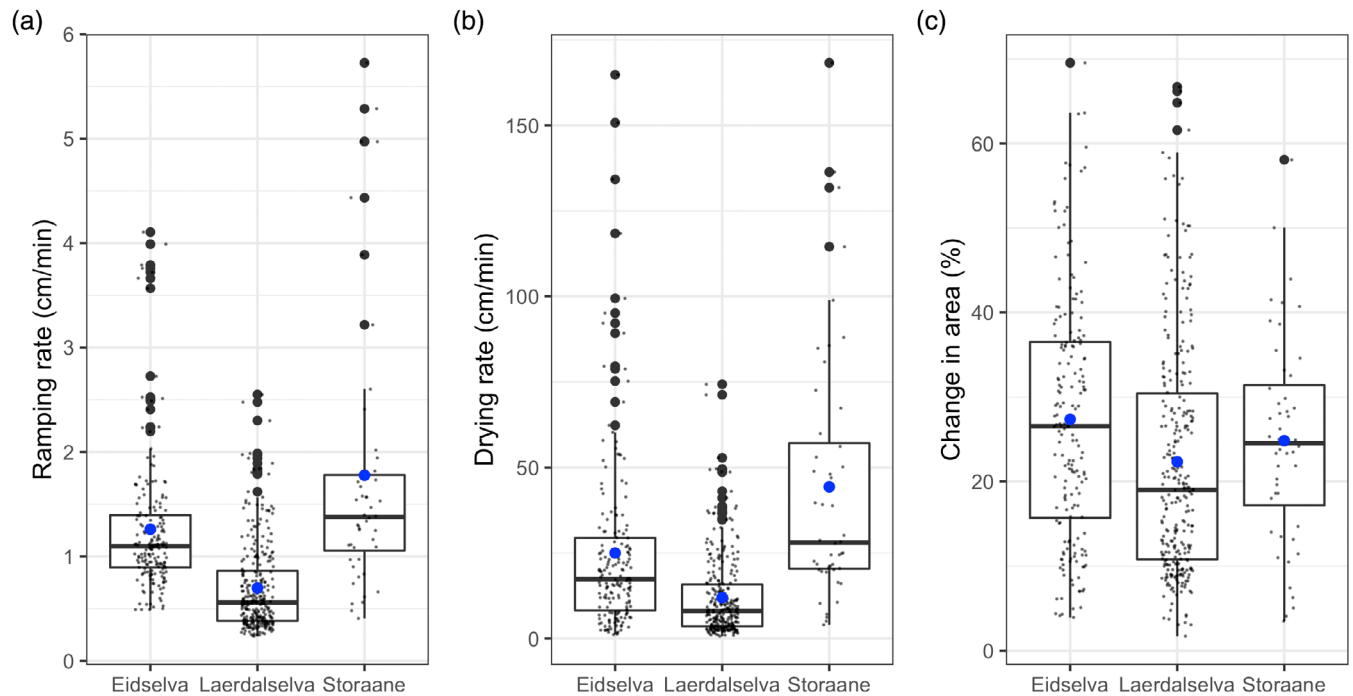

FIGURE 7 Overview of key stranding indices for the three rivers, (a) vertical ramping rate (cm/min), (b) lateral drying rate (cm/min), and (c) dry area from full to low flow (%). The blue marker represents the mean. [Color figure can be viewed at wileyonlinelibrary.com]
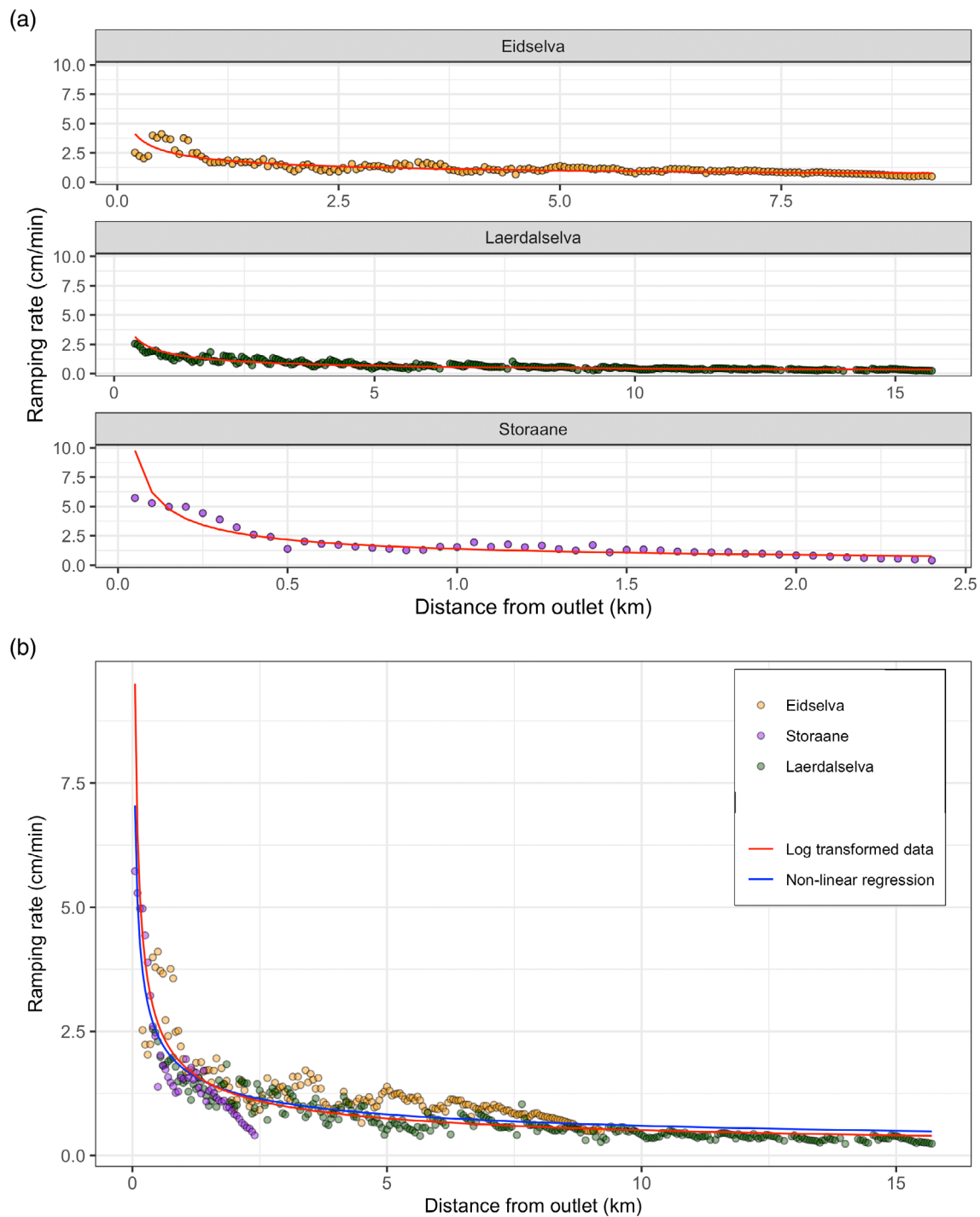
(a)

(b)

FIGURE 8 (a) Ramping rate as a function of the distance from the hydropower outlet. The red line shows the fitted relationship between the ramping rate and distance from the outlet. (b) Ramping rate for all rivers with fitted curves using the linear regression on log-transformed data and a non-linear regression method. Note the variation in the x-axis in panel (a). [Color figure can be viewed at wileyonlinelibrary.com]

and reduces the goodness of fit. The longitudinal slope is significant ($p = 0.017$) but gives no increase in goodness of fit. Adding the distance from the outlet to the equation has a significant contribution ($p < 0.01$) and increased R^2 to 0.68. Further adding an interaction term between the distance from the outlet and the mean cross-sectional slope increased the goodness of fit to 0.72. The mean slope and the distance from the outlet show a low correlation. Adding the

depth-to-width ratio as a secondary explanatory variable had no effect and was not significant, but in combination with the distance from the outlet this was significant but without adding to the goodness of fit. Adding the river as a random effect in the analysis did improve the result for the lateral drying rate indicating that the difference between the rivers is a factor in explaining the relation between the lateral drying rate and the physical features of the reaches.
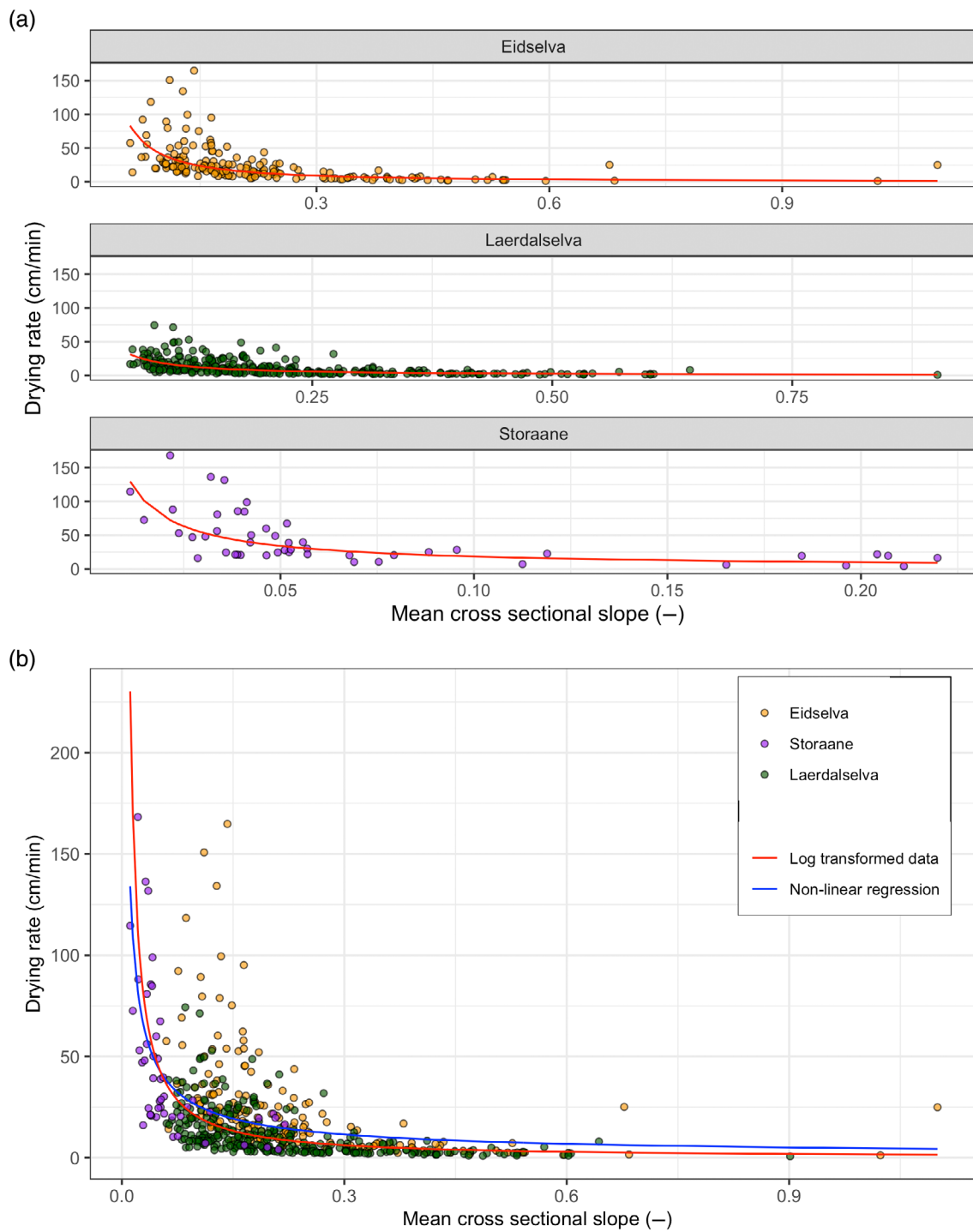
(a)

(b)

FIGURE 9 (a) Lateral drying rate as a function of the mean cross-sectional slope for the three study sites with fitted regression line. (b) Lateral drying rate for all rivers with linear regression on log-transformed data non-linear fitted models. Note the variation in the x-axis in panel (a). [Color figure can be viewed at wileyonlinelibrary.com]

To see if varying river lengths influenced the result, we shortened all rivers to the length of Storåne (the shortest of the study sites) and ran the same kind of analysis on the reduced dataset. There is still a significant relationship with the distance from the outlet, but the goodness of fit is reduced compared to the full dataset ($p < 0.001$, $R^2 = 0.67$). Adding the river width as a second explanatory variable has a significant impact ($p < 0.01$) in this case and a larger impact on the increase of the goodness of fit than in the case where all data is included (R^2 increases to 0.76). The sign shows that an increasing river width decreases the vertical ramping rate.

4 | DISCUSSION

In this paper, we investigated the lateral drying rate and the vertical ramping rate for simulated turbine stops in three different rivers using 2D hydraulic modeling. The simulations were based on detailed DEMs from bathymetric LiDAR providing a basis for evaluation of stranding indexes with high spatial detail. We computed several descriptors of the river geometry both transverse and longitudinally and related the hydropeaking indices to geometric descriptors through statistical analysis. A dampening effect on the ramping rate is seen as we move downstream of the power plant in each of the study rivers and when all data is pooled into one dataset. A relationship between the cross-sectional shape and the distance from the outlet for the lateral drying rates was found for both individual rivers and for the pooled dataset.

The analysis is to a large extent based on hydraulic simulations and uncertainties in the simulations and underlying bathymetry will influence the result. But with the high precision bathymetric data used, and the calibration done we do think the results are reliable also in the detail needed for assessment of dried areas (In Lærdal, a comparison of observed and modeled wetted areas for the discharge during the LiDAR flight had an average error of 1.5% (Alfredsen et al., 2019). In Storåne, a comparison of modeled water level with GPS-measured water level had an average error of 1.5 cm). The evaluation of the hydraulic model for Eidselva was done mainly by visual comparison against simulated aerial images since no other data is available. This analysis therefore has uncertainties in the subjective evaluation of the riverbanks and since overhanging trees or shade effects obscures a clear view of the bank in some areas. We still think this provides a reliable calibration of the model of Eidselva, which is supported by the experiences from Storåne and Lærdal where a comparison with images was supported by a quantitative assessment from measured water levels and water surface extents (Alfredsen et al., 2019; Juarez et al., 2019). The hydropeaking indices computed for the three rivers in this study do show that the hydropeaking regimes we have used all is above critical limits both for ramping rate and for the change of wetted area if measured against the limits in Bakken et al. (2021), and can be considered as examples of severe hydropeaking. The analysis identified clear relations between the hydropeaking indices and features of the rivers. The vertical ramping rate is mainly explained by the dampening as we move downstream from the outlet. When rivers are evaluated with the same river length, the river width shows an increased importance in predicting the vertical ramping rate. This indicates that the importance of the river width is not properly revealed in the full dataset and that there is a source of uncertainty when combining various river lengths. That river width should have an impact on the dampening of the wave is in line with what should be expected since retention is most likely higher and the drop in water level that corresponds to a drop in discharge is smaller in a wide river. The magnitude of the lateral drying rate is explained mainly by the slope of the riverbanks which is as expected since a mild sloped cross section will expose more dried-out areas than a steep-sided cross section when the water level is being reduced. From the analysis, we also see an effect of the distance from the outlet on

the dried rate which may translate into the location in the river, but the effect of the combination of these variables is not very clear. In this work, easily obtained river features have been used to try to explain potential stranding sites and we have not considered the detailed morphology which is important for stranding assessment (Hauer et al., 2014). Another important factor not evaluated in this study is the river substrate which will be an important additional factor in determining if an area should be considered an important habitat or not in an assessment of hydropeaking severity. Such data, if available, could be combined with the assessment above to further pinpoint critical locations.

Stranding of fish has been related to the vertical ramping rate in several studies (e.g., Halleraker et al., 2003; Moreira et al., 2019), and restrictions on the ramping rate are also used in mitigating negative effects of hydropeaking (Halleraker et al., 2022). There has been less focus on the effect of high lateral drying rates on the riverbanks, and according to Moreira et al. (2019) no specific criteria to avoid lateral drying is defined in the literature. However recent results (e.g., Hauer et al., 2023) show that this is an important measure of the effect of hydropeaking operations. Here, we have assessed both these hydropeaking indices and see that the fitted statistical model fits well to the vertical ramping rate and provides a reasonable explanation of the lateral ramping rate.

A dampening of the ramping rate is seen in all our study sites as we progress downstream from the outlet, which can be related to the dampening effect of the morphological features of the river. Similar dampening is seen also by Burman et al. (2021) who modeled how the duration and frequency of turbine stop propagated in a bypass channel in the Ume River, by Hauer et al. (2017) in a study in the Drau River in Austria and by Alfredsen et al. (2022) in a study in Nidelva in Norway. Compared to the study by Hauer et al. (2017), we also see comparable magnitudes of ramping. Related to the lateral drying rate, Hauer et al. (2017) computed the lateral drying rate for the Drau River and found large variability. Our study see that sections with a high lateral drying rate do not necessarily coincide with the sections with a high vertical ramping rate, and this is consistent with the findings of Hauer et al. (2017). This is an interesting finding and it also indicates that the ramping rate should be complemented by the lateral drying rate as a measure of hydropeaking severity. This is also discussed by Le Coarer et al. (2022) and in a study by Hauer et al. (2023) the lateral drying rate is used in a study on changes in hydropeaking effects when the river bathymetry is changing. In our study, the lateral drying rate is computed in a dense set of cross sections along the river, while Le Coarer et al. (2022) present a method to compute the lateral drying rate in larger spatial detail which could be very useful for a detailed assessment of habitat at risk during hydropeaking. To fully utilize the lateral drying rate data on stranding of fish or other species needs to be collected and critical levels should be developed.

Norway has a large number of power plants with outlets in rivers and a considerable length of river potentially influenced by hydropower production (Halleraker et al., 2022). The morphology of the potentially affected rivers varies, but the three rivers used here should be representative of many gravel bed rivers with varying degrees of

embankment structures which is common in Norway. Further, the Norwegian hydropower system with high storage capacity and a large potential for hydropeaking operation is ideally suited for balancing a growing amount of non-storable renewable energy, and this is a use of hydropower that is outlined in the scenarios for future power generation. For just a few of the river's downstream of power plants there are bathymetric data of adequate detail to do a similar detailed hydraulic assessment on consequences of hydropeaking as has been shown here, and there is a need to find ways to evaluate potential impacts based on less complex methods. The relation between the physical characteristics and hydropeaking indices seen in this study could be a way to do an initial evaluation of the impact of hydropeaking operation in a screening of sites that could be used for hydropeaking operation. Even if bathymetric data does not exist for a specific river, access to detailed topographic data of the river valley is available in many places (in Norway through the www.hoydedata.no repository), and such data could be used to estimate the river width, the distance from the outlet and the channel side slope for the initial assessment of hydropeaking impacts. The combination of drone imagery and Structure for Motion photogrammetry is also a possible method to get data for an initial assessment of hydropeaking severity using the relations found in this study. In addition to finding sites where hydropeaking operation could lead to severe problems, it can also be used in a screening process to identify areas where flexible operation of power plants potentially could be done with as little harm as possible and thereby find sites where data could be collected, and more detailed assessments could be carried out.

5 | CONCLUSION

Hydropeaking operations can have severe effects on the ecology of rivers, and the assessment of impacts is needed. The lack of detailed bathymetric data to do detailed assessments is common in many places, and here we propose a method for an initial screening of possible impacts from developing hydropeaking based on descriptors on river geometry that can be derived from topographic data.

DATA AVAILABILITY STATEMENT
Access to LiDAR data through the repository of the Norwegian Mapping Authority, www.hoydedata.no.

ORCID
Knut Alfredsen https://orcid.org/0000-0002-4076-8351

REFERENCES

Alfredsen, K., Juarez, A., Kenawi, M., Graf, M., & Saha, S. (2022). Mitigation of environmental effects of frequent flow ramping scenarios in a regulated river. *Frontiers in Environmental Science*, 10, 944033. https://doi.org/10.3389/fenvs.2022.944033

Alfredsen, K., Juarez, A., Limpens, E., & Sivakumar, A. (2019). *Simulering av vassdekt areal i Lærdalselva. (Simulation of water covered area in Lærdalselva)*. Norwegian University of Science and Technology B1-2019-5.

Ashraf, F., Haghighi, A., Riml, J., Alfredsen, K., Koskela, J., Kløve, B., & Marttila, H. (2018). Changes in short term river flow regulation and hydropeaking in Nordic rivers. *Scientific Reports*, 8, 17232. https://doi.org/10.1038/s41598-018-35406-3

Awadallah, M., Juarez, A., & Alfredsen, K. (2022). Comparison between topographic and bathymetric LiDAR terrain models in flood inundation estimations. *Remote Sensing*, 14(1), 227. https://doi.org/10.3390/rs14010227

Bakken, T. H., Harby, A., Forseth, T., Ugedal, O., Sauterleute, J., Halleraker, J. H., & Alfredsen, K. (2021). Classification of hydropeaking impacts on Atlantic salmon populations in regulated rivers. *River Research and Applications*, 39, 313–325. https://doi.org/10.1002/rra.3917

Bates, D., Maechler, M., Bolker, B., & Walker, S. (2015). Fitting linear mixed-effects models using lme4. *Journal of Statistical Software*, 67(1), 1–48.

Bejarano, M., Garcia-Palacios, J., Sordo-Ward, A., Garrote, L., & Nilsson, C. (2020). A new tool for assessing environmental impacts of altering short-term flow and water level regimes. *Water*, 12(10), 2913. https://doi.org/10.3390/w12102913

Bejarano, M., Jansson, R., & Nilsson, C. (2017). The effects of hydropeaking on riverine plants: A review. *Biological Reviews*, 93(1), 658–673. https://doi.org/10.1111/brv.12362

Bejarano, M., Sordo-Ward, A., Alonso, C., & Nilsson, C. (2017). Characterizing effects of hydropower plants on sub-daily flow regimes. *Journal of Hydrology*, 550, 186–200.

Berland, G., Nickelsen, T., Heggenes, J., Økland, F., Thorstad, E. B., & Halleraker, J. H. (2004). Movements of wild Atlantic salmon parr in relation to peaking flows below a hydro power station. *Rivers Research and Applications*, 20(8), 957–966.

Bevelhimer, M., McManamay, R., & O'Connor, B. (2014). Characterising sub-daily flow regimes: Implications of hydrologic resolution on ecohydrology. *River Research and Applications*, 31, 867–879. https://doi.org/10.1002/rra.2781

Brunner, G. (2021). HEC-RAS river analysis system US army corps of engineers CPD-68.

Bruno, M., Siviglia, A., Carolli, M., & Maiolini, B. (2013). Multiple drift responses of benthic invertebrates to interacting hydropeaking and thermopeaking waves. *Ecohydrology*, 6(4), 511–522. https://doi.org/10.1002/eco.1275

Bürgler, M., Vetsch, D., Boes, R., & Vanzo, D. (2022). Systematic comparison of 1D and 2D hydrodynamic models for the assessment of hydropeaking alterations. *River Research and Applications*, 39(3), 460–477. https://doi.org/10.1002/rra.4051

Burman, A., Hedger, R., Hellström, J., Andersson, A., & Sundt-Hansen, L. (2021). Modelling the downstream longitudinal effects of frequent hydropeaking on the spawning potential and stranding susceptibility of salmonids. *Science of the Total Environment*, 796, 148999. https://doi.org/10.1016/j.scitotenv.2021.148999

Carolli, M., Vanzo, D., Siviglia, A., Zolezzi, G., Bruno, M., & Alfredsen, K. (2015). A simple procedure for the assessment of hydropeaking flow alterations applied to several European streams. *Aquatic Sciences*, 77(4), 639–653. https://doi.org/10.1007/s00027-015-0408-5

Casas-Mulet, R., Alfredsen, K., Boissy, T., Sundt, H., & Rüther, N. (2014). Performance of a one-dimensional hydraulic model for the calculation of stranding areas in hydropeaking rivers. *Rivers Research and Applications: An International Journal Devoted to River Research and Management*, *31*, 143–155. https://doi.org/10.1002/rra.2734

Charmasson, J., & Zinke, P. (2011). Mitigation measures against hydropeaking effects SINTEF energy AS SINTEF report TR A7 192 51.

Greimel, F., Zeiringer, B., Höller, N., Grün, B., Godina, R., & Schmutz, S. (2016). A method to detect and characterize sub-daily flow fluctuations. *Hydrological Processes*, *30*, 2063–2078. https://doi.org/10.1002/hyp.10773

Halleraker, J. H., Kenawi, M., L'Abée-Lund, J., Bakken, T. H., & Alfredsen, K. (2022). Assessment of flow ramping in water bodies impacted by hydropower operation in Norway—Is hydropower with environmental restrictions more sustainable? *Science of the Total Environment*, *832*, 154776. https://doi.org/10.1016/j.scitotenv.2022.154776

Halleraker, J. H., Saltveit, S. J., Harby, A., Arnekleiv, J. V., Fjeldstad, H.-P., & Kohler, B. (2003). Factors influencing stranding of wild juvenile brown trout (*Salmo trutta*) during rapid and frequent flow decreases in an artificial stream. *River Research and Applications*, *19*, 589–603.

Hauer, C., Holzapfel, P., Leitner, P., & Graf, W. (2017). Longitudinal assessment of hydropeaking impacts on various scales for an improved process understanding and the design of mitigation measures. *Science of the Total Environment*, *575*, 1503–1514. https://doi.org/10.1016/j.scitotenv.2016.10.031

Hauer, C., Schmalfuss, L., Unfer, G., Schletterer, M., Fuhrmann, M., & Holzapfel, P. (2023). Evaluation of the potential stranding risk for aquatic organisms according to long-term morphological changes and grain size in alpine rivers impacted by hydropeaking. *Science of the Total Environment*, *883*, 163667. https://doi.org/10.1016/j.scitotenv.2023.163667

Hauer, C., Unfer, G., Holzapfel, P., Haimann, M., & Habersack, H. (2014). Impact of channel bar form and grain size variability on estimated stranding risk of juvenile brown trout during hydropeaking. *Earth Surface Processes and Landforms*, *39*, 1622–1641. https://doi.org/10.1002/esp.3552

Hayes, D., Moreira, M., Boavida, I., Haslauer, M., Unfer, G., Zeiringer, B., Greimel, F., Auer, S., Ferreira, T., & Schmutz, S. (2019). Life stage-specific hydropeaking flow rules. *Sustainability*, *11*(6), 1547. https://doi.org/10.3390/su11061547

Juarez, A., Adeva-Bustos, A., Alfredsen, K., & Dønnum, B. (2019). Performance of a two-dimensional hydraulic model for the evaluation of stranding areas and characterization of rapid fluctuations in hydropeaking rivers. *Water*, *11*, 26. https://doi.org/10.3390/w11020201

Larrieu, K., Pasternack, G., & Schwindt, S. (2020). Automated analysis of lateral river connectivity and fish stranding risks-part 1: Review, theory and algorithm. *Ecohydrology*, *14*, e2268. https://doi.org/10.1002/eco.2268

Le Coarer, Y., Lizée, M.-H., Beche, L., & Logez, M. (2022). Horizontal ramping rate framework to quantify hydropeaking stranding risk for fish. *River Research and Applications*, *39*, 478–489. https://doi.org/10.1002/rra.4087

Mandlburger, G., Hauer, C., Wiesner, M., & Pfeifer, N. (2015). Topo-bathymetric LiDAR for monitoring river morphodynamics and instream habitats—A case study at the Pielach River. *Remote Sensing*, *7*, 6190–6195. https://doi.org/10.3390/rs70506160

Moreira, M., Hayes, D., Boavida, I., Schletterer, M., Schmutz, S., & Pinheiro, A. (2019). Ecologically-based criteria for hydropeaking mitigation: A review. *Science of the Total Environment*, *657*, 1508–1522. https://doi.org/10.1016/j.scitotenv.2018.12.107

Padfield, D., & Matheson, G. (2020). nls.multstart: Robust non-linear regression using AIC scores.

R Core Team. (2019). *R: A language and environment for statistical computing*. R Foundation for Statistical Computing.

Saltveit, S. J., Brabrand, Å., Juarez, A., Stickler, M., & Dønnum, B. (2020). The impact of hydropeaking on juvenile brown trout (*Salmo trutta*) in a Norwegian regulated river. *Sustainability*, *12*(20), 8670. https://doi.org/10.3390/su12208670

Saltveit, S. J., Halleraker, J. H., Arnekleiv, J. V., & Harby, A. (2001). Field experimentson stranding in juvenile Atlantic salmon and brown trout during rapid flow decreases caused by hydropeaking. *Regulated Rivers: Research and Management*, *17*, 609–622.

Sauterleute, J., & Charmasson, J. (2014). A computational tool for characterisation of rapid fluctuations in flow and stage in rivers caused by hydropeaking. *Environmental Modelling and Software*, *55*, 266–278.

Schmutz, S., Bakken, T. H., Friederich, T., Greimel, F., Harby, A., Jungwirth, M., Melcher, A., Unfer, G., & Zeiringer, B. (2015). Response of fish communities to hydrological and morphological alterations in hydropeaking rivers of Austria. *River Research and Applications*, *31*, 919–930. https://doi.org/10.1002/rra.2795

Scruton, D. A., Pennel, C., Ollerhead, L. M. N., Alfredsen, K., Stickler, M., Harby, A., Robertson, M. J., Clarke, K. D., & LeDrew, L. (2008). A synopsis of hydropeaking studies on the response of juvenile Atlantic salmon to experimental flow alteration. *Hydrobiologia*, *609*, 263–275. https://doi.org/10.1007/s10750-008-9409-x

Stickler, M., Dåsnes, H., Malmuist, C., Moe, J., Borge, A. F., Fritsvold, L., Øie, M., Sandøy, S., & Dønnum, B. O. (2023). Validation and application of Airborne LiDAR Bathymetry (ALB) technology for improved management and monitoring of Norwegian rivers and lakes. NVE/Kartverket ISBN 978-82-410-2181-7.

Vanzo, D., Tancon, M., Zolezzi, G., Alfredsen, K., & Siviglia, A. (2016). A modeling approach for the quantification of fish stranding risk: The case of Lundesokna river (Norway). 11th ISE.

Wickham, H. (2016). *ggplot2: Elegant graphics for data analysis*. Springer-Verlag.

SUPPORTING INFORMATION

Additional supporting information can be found online in the Supporting Information section at the end of this article.